

# 1 Using climate to relate water-discharge 2 and area in modern and ancient 3 catchments

---

4 Christian Haug Eide\*<sup>1</sup>, Reidar Müller<sup>2</sup> and William Helland-Hansen<sup>1</sup>

5 <sup>1</sup>Department of Earth Science, University of Bergen, Norway

6 <sup>2</sup>Department of Geosciences, University of Oslo, Norway

7 \*Correspondence: christian.eide@uib.no

8

9 *This is a preprint for a manuscript submitted to the journal Sedimentology.*

10 *The peer-reviewed version-on-record can be found here: <https://dx.doi.org/10.1111/sed.12426>*

11

12 Running head: Relating water-discharge and catchment area

13 Supplementary material: A1, Spreadsheets used for calculations and plots. A2, Cross-plots and  
14 regression lines to determine values for  $k$  and  $m$  by runoff class; Find the data here:

15 <https://onlinelibrary.wiley.com/doi/abs/10.1111/sed.12426>

16

17 **Abstract**

18 Models relating sediment-supply to catchment-properties are important in order to use the  
19 geological record to deduce landscape evolution and the interplay between tectonics and climate.  
20 Water-discharge ( $Q_w$ ) is an important factor in the widely used BQ<sub>w</sub>ART-model of Syvitski and  
21 Milliman (2007), which relates sediment load to a set of measurable catchment parameters.  
22 Although many of the factors in this equation may be independently estimated with some degree of  
23 certainty in ancient systems, water-discharge ( $Q_w$ ) certainly cannot. An analysis of a world database  
24 of modern catchments (Milliman and Farnsworth, 2011) shows that the commonly applied equation  
25 relating catchment area (A) to water-discharge ( $Q_w=0.075A^{0.8}$ ), does not predict water-discharge  
26 from catchment area well in many cases ( $R^2=0.5$  and an error spanning 4 orders-of-magnitude).  
27 Neither does the equation incorporate the effect of arid and wet climate on this relationship. The  
28 inclusion of climate-data into such estimations is an opportunity to refine these estimates, because  
29 generalized estimates of palaeoclimate can often be deduced on the basis of sedimentological data  
30 such as palaeosol types, mineralogy and palaeohydraulics.

31 This paper investigates how the relationship between catchment size and river discharge vary with  
32 four runoff categories (arid, subarid, humid, and wet) which are recognizable in the geological  
33 record, and modify the coefficient and exponent of the abovementioned equation according to these  
34 classes. It follows from this analysis that water-discharge from arid catchments is so variable, that  
35 water-discharge cannot be predicted from catchment area. Our modified model yields improved  
36 results in relating discharge to catchment size ( $R^2=0.95$  and error spanning 1 order-of-magnitude)  
37 when core-, outcrop- or regional palaeoclimate reconstruction data are available in non-arid systems.  
38 In conclusion, this model, in contrast to the previous, is sufficient for many geological applications  
39 and will lead to a higher degree of confidence in the application of mass-balance models in ancient  
40 systems.

41

## 42 1. Introduction

43 The extent and quality of geomorphological and subsurface datasets in the geosciences has increased  
44 greatly in recent decades, and has made it possible to attempt to reconstruct ancient sedimentary  
45 systems from source-to-sink (e.g. Sømme et al., 2009; Allen et al., 2013; Michael et al., 2013;  
46 Hampson et al., 2014; Holbrook and Wanas, 2014, Helland-Hansen et al., 2016). The goal of such  
47 studies is to understand the coupling between sediment producing catchments (or *source* areas),  
48 sediment-storing sedimentary basins (or *sinks*), the sediment routing systems connecting these  
49 systems, and how these interact to record earth history. Such studies may be undertaken to predict  
50 or estimate parameters of sedimentary transport networks which are inaccessible to study due to  
51 erosion or burial (Martinsen et al., 2010), understanding propagation and fidelity of environmental  
52 signals through time (Paola et al., 1992; Romans et al., 2016), and the evolution of past landscapes  
53 (e.g. Sømme et al., 2009; Bhattacharya et al., 2015).

54 In deep-time systems ( $\gg 10^6$  Ma), significant parts of sediment sinks are often preserved in  
55 sedimentary basins, but the sediment source areas are commonly eroded or extensively modified  
56 (e.g. Blum and Pecha, 2014; Eide et al., 2016). Ancient catchment areas may be reconstructed to  
57 some degree using different thermochronological methods, such as detrital zircon and fission track  
58 data (e.g. Gallagher et al., 1998; Fedo et al., 2003; Lisker et al., 2009). However, these methods  
59 require significant skill, time, funds and material. Thus, one of the most popular and well-established  
60 methods used to investigate source-to-sink relationships in ancient systems, is to use the  $BQ_wART$ -  
61 method developed through analysis of modern systems by Syvitski and Milliman (2007) (e.g. Weight  
62 et al., 2011; Sømme et al., 2013). It is an empirical model, based on global regression of modern  
63 catchment data, and uses the following equation for catchments with average mean temperatures  $>$   
64  $2^\circ\text{C}$ :

$$65 \text{ Eq. 1: } Q_s = \omega B Q_w^{0.31} A^{0.5} R T$$

66 where  $Q_s$  is sediment load (Mt/yr),  $\omega$  is a constant of proportionality set to 0.0006,  $Q_w$  is long term  
67 water-discharge ( $\text{km}^3/\text{yr}$ ),  $A$  is catchment area ( $\text{km}^2$ ),  $R$  is maximum relief in the catchment (km),  $T$  is  
68 long-term average temperature in the catchment ( $^\circ\text{C}$ ) and  $B$  is a factor based on proportion of  
69 catchment covered by glaciers ( $A_g$ ), lithology ( $L$ ), trapping efficiency of lakes and reservoirs ( $T_e$ ), and  
70 human-influenced soil erosion ( $E_h$ ). In non-glaciated, pre-human catchments, the factor  $B$  simplifies  
71 to lithology ( $L$ ) only. Some inherent limitations to this model should be pointed out: it only includes  
72 suspended load (which is commonly taken to be  $> 90\%$  of total load), and that it is based on time  
73 series in the order of 30 years, and thus underestimates sediment transport related to rare,  
74 catastrophic events (Milliman and Farnsworth, 2011).

75 For ancient catchments, factors such as relief, bedrock type, catchment palaeotemperature and  
76 extent and presence of glaciers may often be approximated based on regional geological evidence,  
77 and from published global data. Relief ( $R$ ) may be estimated through modern topographic analogs  
78 (systems draining uplifted rift shoulders, flat plains or, large orogens), fission track analysis and  
79 preserved palaeosurfaces (e.g. Leturmy et al., 2003; Sømme et al., 2009). Bedrock type ( $L$ ) may be  
80 estimated through provenance studies of detrital mineralogy and clast composition, and  
81 extrapolation of geological maps into now eroded areas. Catchment temperature ( $T$ ) may be  
82 estimated from global palaeo-general circulation models (e.g. Sellwood and Valdes, 2006), isotope-  
83 based palaeotemperature-estimates (Sun et al., 2012), reconstructions based on plant communities  
84 and palynofloras (e.g. Paterson et al., 2015), and geological evidence such as palaeosol types (e.g.

85 Wright, 1990, Mack and James, 1994; Kraus, 1999, Retallack, 2001; Müller et al., 2004; Nystuen et al.,  
86 2014).

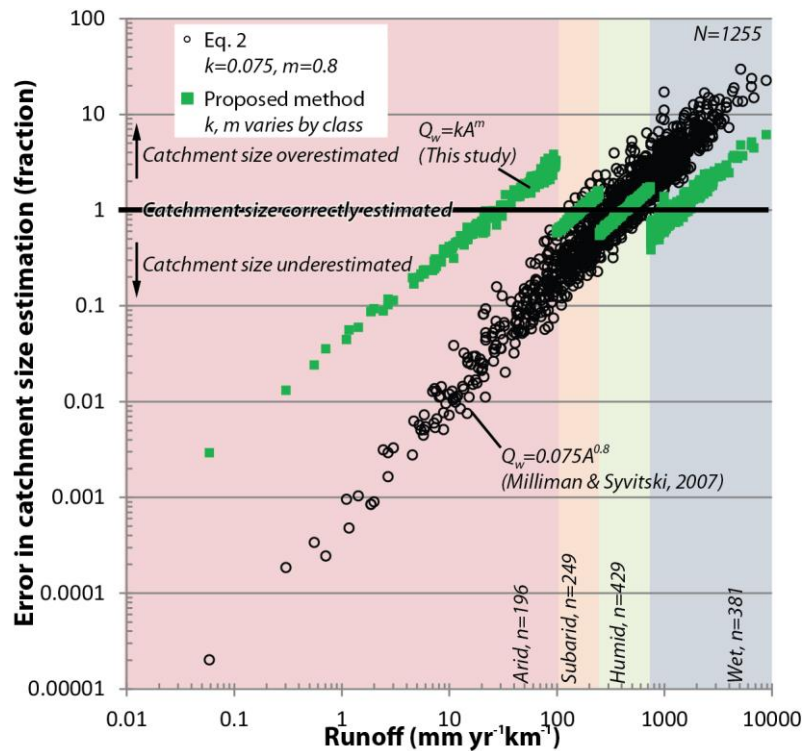
87 In uplifted, dissected and well-exposed systems, water-discharge ( $Q_w$ ) may be estimated using  
88 palaeohydraulic methods based on exposed trunk river channel dimensions (Bhattacharya and Tye,  
89 2004; Holbrook and Wanas, 2014). Although attribute maps derived from 3D-seismic data may give  
90 full plan view control of parts of fluvial systems in the subsurface, wells and 3D-seismic data are  
91 commonly too sparse and too poorly resolved to assess true width and thickness of channels and  
92 barforms. Estimation of water-discharge in the subsurface is thus extremely challenging.

93 Catchment area ( $A$ ) is in most cases hard to constrain accurately in ancient systems, due to erosional  
94 and tectonic modification. Systems with a marked topographic axis, such as in convergent and  
95 transpressive regimes, catchment size may be estimated using distance to the topographic axis and  
96 Hack's Law (Hack, 1957; Rigon et al., 1996). However, these are also the most short lived and  
97 unstable source-to-sink systems, and sediment transport networks are prone to change through time  
98 (Woodcock, 2004). In most other basin types, catchment area ( $A$ ) and water-discharge ( $Q_w$ ) are  
99 difficult to estimate.

100 This presents a problem, because application of the  $BQ_w$ ART-model (Eq. 1) to ancient systems yields  
101 one equation and two poorly constrained unknowns, significantly hampering the usability of this  
102 method. In order to relate these variables, Syvitski and Milliman (2007) presented the following  
103 equation:

$$\text{Eq. 2: } Q_w = kA^m$$

104 , where  $Q_w$  is water-discharge,  $A$  is catchment size,  $k$  is an empirical constant set to 0.075, and  $m$  is an  
105 empirical exponent set to 0.8, providing a link between catchment area and river discharge. This  
106 equation is useful as it provides a simple way to relate sediment supply to parameters which are  
107 possible to estimate in the ancient (e.g. Sømme et al., 2013; Allen et al., 2013), and will in this paper  
108 be referred to as *Eq. 2*. However, this equation is clearly inadequate to accurately relate discharge  
109 and catchment size, because two equally large catchments in different climates will have very  
110 different water-discharge, owing to varying amounts of rainfall and evapotranspiration (e.g. Mu et al.  
111 2007). In this paper, using global catchment data compiled by Milliman and Farnsworth (2011), it is  
112 demonstrated that using fixed values for the constant  $k=0.075$  and exponent  $m=0.8$  in *Eq. 2* for all  
113 systems regardless of climate is inadequate in many settings (Fig. 1).  
114



115

116 Fig. 1: Runoff and error in catchment size estimation using the Eq. 2 and the proposed method for 1255 modern  
 117 catchments (Data from Milliman and Farnsworth, 2011). An error value of 1 indicates no error in the catchment  
 118 estimation, and error values of 0.1 and 10 indicate a ten times under- and overestimation of catchment area,  
 119 respectively. Note the large errors associated with wet and arid systems using Eq. 2 (circles), and how this  
 120 improves significantly using the method proposed in this contribution (squares).

121

122 The runoff (ratio of annual river discharge to catchment area) of rivers varies with climate. Runoff of  
 123 rivers is commonly given in  $\text{mm yr}^{-1} \text{ km}^{-2}$ , and is therefore easily compared to catchment-averaged  
 124 rainfall. The runoff efficiency of a catchment is the ratio of runoff to catchment-averaged rainfall, and  
 125 runoff efficiency is commonly lower in drier catchments due to higher evapotranspiration and  
 126 infiltration, and high in wetter catchments due to moister soil (e.g. McCabe and Wolock, 2016). Thus,  
 127 runoff of rivers is strongly dependent upon climate, as a higher precipitation will lead to higher  
 128 runoff due to both increasing the availability of water, but also due to increase in runoff efficiency.

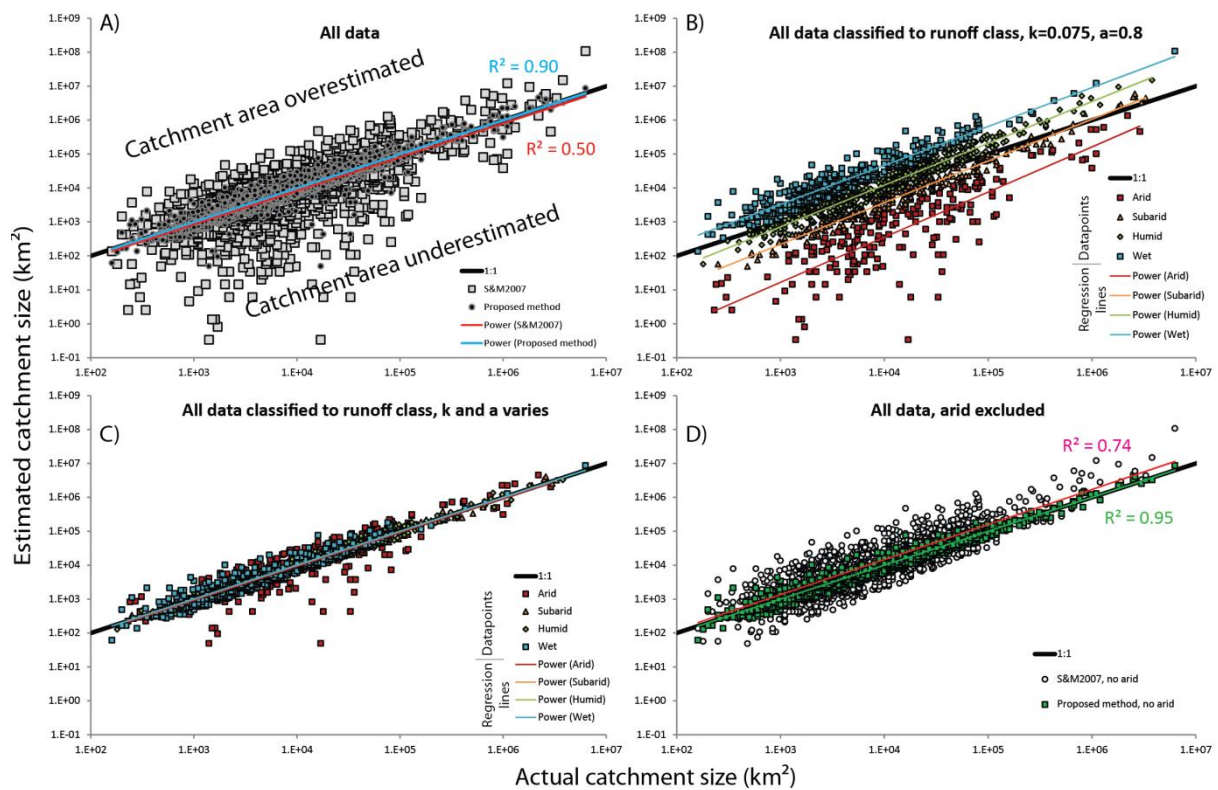
129 Here, it is shown that discharge may be predicted from catchment area (and *vice versa*) at an  
 130 acceptable level of precision and accuracy by choosing appropriate values for  $k$  and  $m$  in Eq. 2 by  
 131 classifying studied deposits into four runoff classes (arid, subarid, humid and wet). These classes can  
 132 readily be estimated by geological palaeoclimatological indicators (e.g. palaeosol types, presence of  
 133 climate-sensitive sedimentary environments such as evaporites and aeolian dunes) and published  
 134 palaeogeographic reconstructions. This yields simple, reliable and well-constrained input to source-  
 135 to-sink models.

136 Thus, the goals of this paper are threefold: (1) to present an improved model for estimating  
 137 relationship between river discharge and catchment for different climate types in modern  
 138 environments, (2) outline how these relationships may be employed in deep time stratigraphic

139 successions where proxies for palaeoclimate can be retrieved, and (3) to investigate in which settings  
 140 this model might be inappropriate.

## 141 2. Dataset and methods

142 This study is based on analysis of the global database of catchment properties presented by Milliman  
 143 and Farnsworth (2011), which collates a wealth of information from modern catchments and their  
 144 sediment supply, such as relief, climate, location, and most importantly for this study, catchment  
 145 area and water-discharge. These systems are investigated using simple cross plots and power law  
 146 regression (Figs. 1 and 2), and are further investigated using published data and publically available  
 147 satellite imagery. The database (Milliman and Farnsworth, 2011) contains 1531 entries, and 1255 of  
 148 these have information about catchment area and river discharge. Furthermore, 72 of these systems  
 149 have information about pre-dam discharge. For these systems, the pre-dam discharge is used to  
 150 provide values for runoff and discharge. It is worth noting that the many of the rivers with pre-dam  
 151 discharge values are well-known rivers with extensive water management systems (e.g. Murray-  
 152 Darling, Nile, Colorado).



153

154 *Fig. 2: Cross plots showing relationship between actual and estimated catchment size using different constants*  
 155 *k and m. Data points are from the catchment database of Milliman and Farnsworth (2011), N=1255. A) Actual*  
 156 *and estimated catchment size using all data and Eq. 2 (squares), compared to all data for the method proposed*  
 157 *herein (circles). (B) Actual and estimated catchment size using all data and Eq. 2, color-coded by runoff class*  
 158 *(arid, subarid, humid and wet). Note the systematic underestimation and large spread of errors in estimation of*  
 159 *arid catchment area, and the systematic overestimation of wet catchment area. (C) Catchment area estimated*  
 160 *using different constant k and exponent m for each runoff class (see Table 1), color-coded by runoff class. Note*  
 161 *the improved fit between actual and estimated runoff compared to (B), and note that errors are still large for*

162 arid systems. (D) Comparison of Eq. 2 and the proposed method, for all data excluding arid systems. S&M2007,  
 163 datapoints using Eq. 2 and  $k=0.075$  and  $m=0.8$  from Syvitski and Milliman, 2007.

164

165 The boundaries for runoff categories employed by Milliman and Farnsworth (2011) in their  
 166 compilation, (arid 0-100; subarid 100-250; humid 250-750; and wet  $>750 \text{ mm km}^{-1} \text{ yr}^{-1}$ ) gave good  
 167 results and are adopted in this study.

168

169 **Table 1:** Runoff category limits, constants  $k$  and  $m$  and coefficients of determination for each of the  
 170 populations plotted in Figure 2.

Model	Class	Runoff ( $\text{mm yr}^{-1} \text{ km}^{-1}$ )	$K$	$m$	$r^2$
Eq. 2 (Syvitski and Milliman, 2007)	<b>All data</b>	<b>&gt;0</b>	<b>0.075</b>	<b>0.8</b>	<b>0.50</b>
	All data, arid excluded	>100	0.075	0.8	0.74
Proposed method (this study)	Arid	0-100	0.0005	1.0633	0.72
	Subarid	100-250	0.0063	0.9824	0.98
	Humid	250-750	0.0161	0.9839	0.96
	Wet	>750	0.0873	0.9164	0.99
	All data	>0	varies	varies	0.90
	<b>All data, arid excluded</b>	<b>&gt;100</b>	<b>varies</b>	<b>varies</b>	<b>0.95</b>

171

172

### 173 3. Results

174 Figure 1 presents the runoff of all systems in the database (Milliman and Farnsworth, 2011), plotted  
 175 against the error of the catchment size estimation. Catchment size estimation is dependent on  
 176 runoff, and is thus systematically greatly underestimated in arid systems (median error: 0.01x),  
 177 systematically underestimated in subarid systems (median error: 0.4x), correctly estimated for humid  
 178 systems, and systematically overestimated for wet systems (median error: 4x).

179 Plots of actual versus estimated catchment size (using Eq. 2 and the coefficients from Syvitski and  
 180 Milliman 2007) also demonstrate this relationship (Fig. 2B): catchment size is underestimated for arid  
 181 systems, and overestimated for wet systems. Furthermore, Eq. 2 leads to large (four orders of  
 182 magnitude) variation in error of estimation of catchment areas for arid systems (Fig. 2B). Subarid,  
 183 humid and wet systems generally show little variation in error and generally constrain the input with  
 184 reasonable accuracy (within 30x).

185

186 In order to obtain new coefficients and exponents for each of the runoff classes, power-law  
 187 regression was performed on cross plots of catchment area versus runoff for each of the four runoff  
 188 classes (Appendix A1). Determined best-fit exponents and coefficients of determination ( $R^2$ ) are  
 189 presented in Table 1. Plots of actual versus estimated catchment size using the proposed model are  
 190 presented in Fig. 2C. These show a significant improvement compared to Eq. 2, but also large  
 191 variations for arid systems. Eq. 2 and the proposed model are compared in Figures 2A and 2D,

192 including and excluding arid systems, respectively. This shows that estimates of catchment size are  
193 significantly improved using the proposed method. However, catchment size estimation appears to  
194 be too variable to be useful in arid catchments.

#### 195 4. Discussion

### 196 **4.1. Recognition of runoff classes in ancient deposits**

197 Defining runoff class of ancient deposits makes estimations of river discharge and catchment area  
198 more accurate (Fig. 2, Table 1). This is possible because runoff is related to features which are  
199 preserved in sedimentary systems (Fig. 3) and observable in the geological record (Table 2). The key  
200 assumption in this work is therefore that the runoff classes defined in this study would correspond to  
201 geologically observable factors, such as the presence of calcretes, coals, particular palaeosol types  
202 and features (e.g. Mack and James, 1994; Bestland, 1997), aeolian dunes, plant communities  
203 (Paterson et al., 2015), soil color, mineralogy, fluvial architectures (Retallack, 2001; Nystuen et al.,  
204 2014), and isotopes (Cerling, 1984). However, care must be taken as climate in the basin can be  
205 different from that in the provenance area (e.g. Nystuen et al., 2014). Furthermore, it must be  
206 pointed out that several of the features mentioned here are not controlled by runoff alone, but are  
207 also partly a function of temperature and evaporation. Models for estimating runoff in cold and polar  
208 systems are not well-developed, and the method presented here would likely not work well in such  
209 systems.



211 *Fig 3: Satellite images of systems in the four categories, showing clearly different landscapes that would be*  
212 *expressed in detectable geological indicators. A) Orange River, Namibia. Runoff =  $4.5 \text{ mm km}^{-1} \text{ yr}^{-1}$ . B) Narmada*  
213 *River, India. Runoff =  $230 \text{ mm km}^{-1} \text{ yr}^{-1}$ . C) Grijalva River, Mexico. Runoff =  $460 \text{ mm km}^{-1} \text{ yr}^{-1}$ . D) Rajang,*  
214 *Indonesia. Runoff =  $2150 \text{ mm km}^{-1} \text{ yr}^{-1}$ . Image data are © Google 2016.*

215

217 **Table 2:** Generalized criteria for determining palaeoclimate from geological indicators.

	<b>Arid</b>	<b>Subarid</b>	<b>Humid</b>	<b>Wet</b>	<b>Notes</b>	<b>References</b>
<b>Runoff (<math>mm\ km^{-1}\ yr^{-1}</math>)</b>	<100	100-250	250-750	>750	-	-
<b>Palaeosol types</b>	Calcisols, gypsisols, entisols, inceptisols	Calcisols, vertisols	Argillisols, spodsols, gleysols, histosols	Histosols, gleysols, Oxisols, agrillisols	Well-drained soils not expected in sedimentary basins in wet and humid systems	Mack and James, 1994
<b>Root types</b>	Deep tap-roots	Deep tap-roots	-	Tabular mat		Retallack, 1997; 2001;
<b>Mineralogy</b>	Presence of gypsum, carbonate.	Presence of carbonate	-	High proportion of quartz versus feldspar,	Quartz/feldspar ratio and ratios of smectite and kaolinite to immature clay minerals (illite and chlorite) increase due to increased chemical weathering under higher temperature and humidity.	Robert and Kennet, 1994; Retallack, 1997; Nystuen et al., 2014;
<b>River architectures</b>	Strongly ephemeral/flashy	Ephemeral/flashy	Perennial	Perennial	-	Tooth, 2000; Nystuen et al., 2014
<b>Other:</b>	Nearby aeolian or evaporite deposits	-	-	-	-	-

218

219

220 **4.2. Comparison to Eq. 2**

221 The comparison of errors in catchment size estimation for Eq. 2 (Eq. 2; Syvitski and Milliman, 2007)  
 222 and the proposed method shows that Eq. 2 performed well in runoff ranges 200-800 mm/km yr (Fig.  
 223 1), a range which contains 43% of the catchments in the database. For the wet category, which  
 224 contains 30% of the data, the proposed method is significantly better than Eq. 2 (Fig. 1). Wet systems  
 225 would commonly be characterized by perennial rivers and abundant gleysols or coal deposits.  
 226 Furthermore, this study shows that it is hard to estimate runoff for arid systems, as annual discharge  
 227 is not primarily controlled by catchment size in such systems. Still, the proposed method decreases  
 228 the error of arid systems by a factor of 100. Finally, this study shows that water-discharge and  
 229 catchment area can be related with a high degree of confidence if the runoff class of the system can  
 230 be determined, with the exception of arid systems.

231 **4.3. Human influence and validity of equations**

232 The majority of world catchments have some degree of human influence. In the database (Milliman  
 233 and Farnsworth, 2011), 72 of the 1254 catchments also have data about pre-dam discharge. 21% of  
 234 these are classified as arid based on runoff, 29% are sub-arid, 31% are humid and 11% are wet. Post-  
 235 dam discharge decrease in 71 of the 72 catchments, and the reduction ranges from 11% (Tapti, India)  
 236 to 99% (Colorado, USA), and no correlation between the amount of decrease and runoff or  
 237 catchment size exists. This indicates that post-dam discharge reduction is mainly determined by  
 238 water management strategies and water demand.

239 It is also worth noting that the rivers with pre-dam discharge-data in the database often represent  
 240 highly populated catchments with well-known and large water management projects, such as the  
 241 Nile, Orange, Los Angeles, Colorado and Huanghe. It may therefore be speculated that discharge  
 242 from catchments without pre-dam discharge data generally is less affected by human intervention

243 than catchments with pre-discharge data. Thus, it is estimated that the coefficients presented here,  
244 which are conditioned to post-dam river discharge, might underestimate final discharge to some  
245 degree. However, further research would be needed to constrain this amount.

## 246 **5. Conclusions**

247 When reconstructing ancient source-to-sink-systems, estimates of water-discharge ( $Q_w$ ) and  
248 catchment area ( $A$ ) are crucial to apply mass-balance models. Here, it is demonstrated that the  
249 previous method ( $Q_w=0.075A^{0.8}$ ) works reasonably well in in subarid and humid settings, but that it  
250 yields a significant overestimation of catchment size in wet systems, and a significant  
251 underestimation of catchment size in arid systems. Because catchment climate can be readily  
252 defined from geological evidence, a new method with different exponent and coefficient for each  
253 runoff class is presented. This study shows that it is possible to achieve improved correspondence  
254 between measured and predicted values ( $r^2$ -values of 0.95) in modern systems. However, arid  
255 systems show too high variability to be reliably predicted in this way.

## 256 **6. Acknowledgements**

257 This work has been funded by the Trias North project under grant 234152 from the Research Council of Norway and with financial support  
258 from Tullow Oil Norge, Lundin Norway, Statoil Petroleum, Edison Norge and Dea Norge. The authors would like to thank all scientists in  
259 general, and J.P.M. Milliman and K.L. Farnsworth in particular, who make full datasets available to the public for the advancement of  
260 science.

261

## 262 7. Captions

263 *Fig. 1: Runoff and error in catchment size estimation using the Eq. 2 and the proposed method for 1255 modern*  
264 *catchments (Data from Milliman and Farnsworth, 2011). An error value of 1 indicates no error in the catchment*  
265 *estimation, and error values of 0.1 and 10 indicate a ten times under- and overestimation of catchment area,*  
266 *respectively. Note the large errors associated with wet and arid systems using Eq. 2 (circles), and how this*  
267 *improves significantly using the method proposed in this contribution (squares).*

268 *Fig. 2: Cross plots showing relationship between actual and estimated catchment size using different constants*  
269 *k and m. Data points are from the catchment database of Milliman and Farnsworth (2011), N=1255. A) Actual*  
270 *and estimated catchment size using all data and Eq. 2 (squares), compared to all data for the method proposed*  
271 *herein (circles). (B) Actual and estimated catchment size using all data and Eq. 2, color-coded by runoff class*  
272 *(arid, subarid, humid and wet). Note the systematic underestimation and large spread of errors in estimation of*  
273 *arid catchment area, and the systematic overestimation of wet catchment area. C) Catchment area estimated*  
274 *using different constant k and exponent m for each runoff class (see Table 1), color-coded by runoff class. Note*  
275 *the improved fit between actual and estimated runoff compared to (B), and note that errors are still large for*  
276 *arid systems. (D) Comparison of Eq. 2 and the proposed method, for all data excluding arid systems. S&M2007,*  
277 *datapoints using Eq. 2 and k=0.075 and m=0.8 from Syvitski and Milliman, 2007.*

278 *Fig 3: Satellite images of systems in the four categories, showing clearly different landscapes that would be*  
279 *expressed in detectable geological indicators. A) Orange River, Namibia. Runoff =  $4.5 \text{ mm km}^{-1} \text{ yr}^{-1}$ . B) Narmada*  
280 *River, India. Runoff =  $230 \text{ mm km}^{-1} \text{ yr}^{-1}$ . C) Grijalva River, Mexico. Runoff =  $460 \text{ mm km}^{-1} \text{ yr}^{-1}$ . D) Rajang,*  
281 *Indonesia. Runoff =  $2150 \text{ mm km}^{-1} \text{ yr}^{-1}$ . Image data are © Google 2016.*

282 **Table 1:** Runoff category limits, constants *k* and *m* and coefficients of determination for each of the  
283 populations plotted in Figure 2.

284 **Table 2:** Generalized criteria for determining palaeoclimate from geological indicators.

285

286

## 287 **8. References**

- 288 Allen, P. A., Armitage, J. J., Carter, A., Duller, R. A., Michael, N. A., Sinclair, H. D., ... & Whittaker, A. C.  
289 (2013). The Qs problem: Sediment volumetric balance of proximal foreland basin  
290 systems. *Sedimentology*, 60(1), 102-130.
- 291 Bestland, E.A., Retallack, G.J. and Swisher, Iii, C.C., 1997. Stepwise climate change recorded in  
292 Eocene-Oligocene paleosol sequences from central Oregon. *The Journal of Geology*, 105(2), pp.153-  
293 172.
- 294 Bhattacharya, J. P., & Tye, R. S. (2004). Searching for modern Ferron analogs and application to  
295 subsurface interpretation. Regional to wellbore analog for fluvial-deltaic reservoir modeling: The  
296 Ferron Sandstone of Utah: AAPG Studies in Geology, 50, 39-57.
- 297 Bhattacharya, J. P., Copeland, P., Lawton, T. F., & Holbrook, J. (2015). Estimation of source area, river  
298 paleo-discharge, paleoslope, and sediment budgets of linked deep-time depositional systems and  
299 implications for hydrocarbon potential. *Earth-Science Reviews*.
- 300 Blum, M., & Pecha, M. (2014). Mid-Cretaceous to Paleocene North American drainage reorganization  
301 from detrital zircons. *Geology*, 42(7), 607-610.
- 302 Cerling, T.E., 1984. The stable isotopic composition of modern soil carbonate and its relation to  
303 climate. *Earth and Planetary Science Letters*, 71, p. 229-240.
- 304 Eide, C. H., Howell, J. A., Buckley, S. J., Martinius, A. W., Oftedal, B. T., & Henstra, G. A. (2016). Facies  
305 model for a coarse-grained, tide-influenced delta: Gule Horn Formation (Early Jurassic), Jameson  
306 Land, Greenland. *Sedimentology*.
- 307 Fedo, C. M., Sircombe, K. N., & Rainbird, R. H. (2003). Detrital zircon analysis of the sedimentary  
308 record. *Reviews in Mineralogy and Geochemistry*, 53(1), 277-303.
- 309 Gallagher, K., Brown, R., & Johnson, C. (1998). Fission track analysis and its applications to geological  
310 problems. *Annual Review of Earth and Planetary Sciences*, 26(1), 519-572.
- 311 Hack, J. T. (1957). Studies of longitudinal profiles in Virginia and Maryland, U.S. Geol. Surv. Prof. Pap.,  
312 294-B, 1, 1957.
- 313 Hampson, G. J., Duller, R. A., Petter, A. L., Robinson, R. A., & Allen, P. A. (2014). Mass-Balance  
314 Constraints On Stratigraphic Interpretation of Linked Alluvial–Coastal–Shelfal Deposits From Source  
315 To Sink: Example From Cretaceous Western Interior Basin, Utah and Colorado, USA. *Journal of*  
316 *Sedimentary Research*, 84(11), 935-960.
- 317 Helland-Hansen, W., Sømme, T. O., Martinsen, O. J., Lunt, I., & Thurmond, J. (2016). Deciphering  
318 Earth's natural hourglasses: Perspectives on source-to-sink analysis. *Journal of Sedimentary*  
319 *Research*, 86, 1-26. <http://dx.doi.org/10.2110/jsr.2016.56>
- 320 Holbrook, J., & Wanas, H. (2014). A fulcrum approach to assessing source-to-sink mass balance using  
321 channel paleohydrologic parameters derivable from common fluvial data sets with an example from  
322 the Cretaceous of Egypt. *Journal of Sedimentary Research*, 84(5), 349-372.

- 323 Kraus, M. (1999) Paleosols in clastic sedimentary rocks: their geologic applications. *Earth-Sci.*  
324 *Rev.*, 47, 41-70.
- 325 Leturmy, P., Lucazeau, F., & Brigaud, F. (2003). Dynamic interactions between the Gulf of Guinea  
326 passive margin and the Congo River drainage basin: 1. Morphology and mass balance. *Journal of*  
327 *Geophysical Research: Solid Earth*, 108(B8).
- 328 Lisker, F., Ventura, B. and Glasmacher, U.A., 2009. Apatite thermochronology in modern geology.  
329 Geological Society, London, Special Publications, 324(1), pp.1-23.
- 330 Mack, G. H., & James, W. C. (1994). Paleoclimate and the global distribution of paleosols. *The Journal*  
331 *of Geology*, 360-366.
- 332 Martinsen, O. J., Sømme, T. O., Thurmond, J. B., Helland-Hansen, W., & Lunt, I. (2010). Source-to-sink  
333 systems on passive margins: theory and practice with an example from the Norwegian continental  
334 margin. In Geological Society, London, Petroleum Geology Conference series (Vol. 7, pp. 913-920).  
335 Geological Society of London.
- 336 McCabe, G.J. and Wolock, D.M., 2016. Variability and Trends in Runoff Efficiency in the Conterminous  
337 United States. *JAWRA Journal of the American Water Resources Association*.
- 338 Michael, N. A., Whittaker, A. C., & Allen, P. A. (2013). The functioning of sediment routing systems  
339 using a mass balance approach: Example from the Eocene of the southern Pyrenees. *The Journal of*  
340 *Geology*, 121(6), 581-606.
- 341 Milliman, J. D., & Farnsworth, K. L. (2011). *River discharge to the coastal ocean: a global synthesis*,  
342 Cambridge University Press, Cambridge, UK, 349 pp.
- 343 Mu, Q., Heinsch, F. A., Zhao, M., & Running, S. W. (2007). Development of a global  
344 evapotranspiration algorithm based on MODIS and global meteorology data. *Remote Sensing of*  
345 *Environment*, 111(4), 519-536.
- 346 Müller, R., Nystuen, J.P. and Wright, V.P. (2004) Pedogenic mud aggregates and paleosol  
347 development in ancient dryland river systems: criteria for interpreting alluvial mudrocks and  
348 floodplain dynamics. *J. Sed. Res.*, 74, 537-551.
- 349 Nystuen, J.P., Kjemperud, A.V., Müller, R., Adestål, V. and Schomacker, E.R., 2014. Late Triassic to  
350 Early Jurassic climatic change, northern North Sea region. *From Depositional Systems to Sedimentary*  
351 *Successions on the Norwegian Continental Margin*, pp.59-99.
- 352 Paola, C., Heller, P.L. and Angevine, C.L., 1992. The large-scale dynamics of grain-size variation in  
353 alluvial basins, 1: Theory. *Basin Research*, 4(2), pp.73-90.
- 354 Paterson, N.W., Mangerud, G., Cetean, C.G., Mørk, A., Lord, G.S., Klausen, T.G. and Mørkved, P.T.,  
355 2015. A multidisciplinary biofacies characterisation of the Late Triassic (late Carnian–Rhaetian) Kapp  
356 Toscana Group on Hopen, Arctic Norway. *Palaeogeography, Palaeoclimatology, Palaeoecology*.
- 357 Retallack, G.J., 1997. *Colour guide to paleosols*. John Wiley & Sons Ltd. Chichester, 175 pp.

- 358 Retallack, G.J., 2001. Soils of the past: an introduction to paleopedology. John Wiley & Sons. Oxford,  
359 404 pp.
- 360 Rigon, R., Rodriguez-Iturbe, I., Maritan, A., Giacometti, A., Tarboton, D. G., & Rinaldo, A. (1996). On  
361 Hack's law. *Water Resources Research*, 32(11), 3367-3374.
- 362 Robert, C. and Kennett, J.P., 1994. Antarctic subtropical humid episode at the Paleocene-Eocene  
363 boundary: Clay-mineral evidence. *Geology*, 22(3), pp.211-214.
- 364 Romans, B. W., Castelltort, S., Covault, J. A., Fildani, A., & Walsh, J. P. (2015). Environmental signal  
365 propagation in sedimentary systems across timescales. *Earth-Science Reviews*.
- 366 Sellwood, B. W., & Valdes, P. J. (2006). Mesozoic climates: General circulation models and the rock  
367 record. *Sedimentary geology*, 190(1), 269-287.
- 368 Sun, Y., Joachimski, M.M., Wignall, P.B., Yan, C., Chen, Y., Jiang, H., Wang, L. and Lai, X., 2012. Lethally  
369 hot temperatures during the Early Triassic greenhouse. *Science*, 338(6105), pp.366-370.
- 370 Syvitski, J. P., & Milliman, J. D. (2007). Geology, geography, and humans battle for dominance over  
371 the delivery of fluvial sediment to the coastal ocean. *The Journal of Geology*, 115(1), 1-19.
- 372 Sømme, T. O., Martinsen, O. J., & Lunt, I. (2013). Linking offshore stratigraphy to onshore  
373 paleotopography: The Late Jurassic–Paleocene evolution of the south Norwegian margin. *Geological*  
374 *Society of America Bulletin*, 125(7-8), 1164-1186.
- 375 Sømme, T. O., Martinsen, O. J., & Thurmond, J. B. (2009). Reconstructing morphological and  
376 depositional characteristics in subsurface sedimentary systems: An example from the Maastrichtian–  
377 Danian Ormen Lange system, More Basin, Norwegian Sea. *AAPG bulletin*, 93(10), 1347-1377.
- 378 Tooth, S., 2000. Process, form and change in dryland rivers: a review of recent research. *Earth-*  
379 *Science Reviews*, 51(1), pp.67-107.
- 380 Weight, R.W., Anderson, J.B. and Fernandez, R., 2011. Rapid mud accumulation on the central Texas  
381 shelf linked to climate change and sea-level rise. *Journal of Sedimentary Research*, 81(10), pp.743-  
382 764.
- 383 Woodcock, N.H., 2004. Life span and fate of basins. *Geology*, 32(8), pp.685-688.
- 384 Wright, V.P. (1990) Equatorial aridity and climatic oscillations during the early Carboniferous,  
385 southern Britain. *J. Geol. Soc. London*, 147, 359-363.